Journal of Alloys and Compounds 499 (2010) 43–47

Contents lists available at ScienceDirect

Journal of Alloys and Compounds

journal homepage: www.elsevier.com/locate/jallcom

The manufacture of spherical salt beads and their use as dissolvable templates for the production of cellular solids via a powder metallurgy route

A. Jinnapat, A.R. Kennedy*

Manufacturing Research Division, Faculty of Engineering, University of Nottingham, University Park, Nottingham, NG7 2RD, UK

ARTICLE INFO

Article history:
Received 4 March 2010
Received in revised form 10 March 2010
Accepted 12 March 2010
Available online 18 March 2010

Keywords:
Metals and alloys
Cellular materials
Powder metallurgy
Sintering
Mechanical properties
Microstructure

ABSTRACT

A novel process has been demonstrated for the manufacture of spherical salt beads with sizes between 0.5 and 3.0 mm using a flour-based paste which is mechanically disintegrated in oil. The process has been shown to be repeatable. After thermal decomposition of the flour from the beads they contain a high fraction (16%) of interconnected porosity. Tapped beds of salt beads have been partially filled with an Al alloy powder using vibration. The fine Al powder penetrates the gaps between the salt beads, preserving the structure of the tapped bed, and is a highly attractive alternative to powder mixing methods. After compaction and sintering, and dissolution of the salt, a highly porous component is produced. The porous nature of the beads, which allows water to penetrate them, results in rapid dissolution of the salt from the component. Cellular aluminium parts can be produced with very small deviations in density due to the good control that is possible over the mass fractions of powders that are used and the compaction conditions. The reproducibility in the density results in reproducible mechanical properties.

1. Introduction

Porous metals show unique combinations of properties such as high specific stiffness, low density, high absorption energy, good thermal and electrical conductivity, high damping capacity and good sound absorption. They are used in functional applications such as filters, catalyst supports, heat exchangers, biomedical devices and prostheses and in structural applications where lightweight and energy absorption are needed in the automotive, aerospace, ship building, construction and railway industries [1].

Porous metals can be made by replication methods based on either powder metallurgy (PM) or casting methods. The process for the manufacture of aluminium foams via a PM route typically involves mixing angular salt (NaCl), between 200 and 1000 μm in size, with aluminium powder [2,3]. Due to the large size differences between the salt and the fine Al powder, homogeneous mixing can be difficult to achieve and this can prove to be an obstacle to achieving the interconnecting salt and Al structures that are required. The use of a binder, such as ethanol, methanol, kerosene or water [3], goes some way to minimising segregation of the powders and promoting homogeneous mixing. Salt–Al mixtures are then compressed in order to both define the shape of the part but also to increase inter-particle contact. This is particularly important for the Al powder as extensive deformation ruptures the oxide layer on the powder surfaces, generating fresh metal–metal contact, facilitating successful sintering [4]. Metal powder compacts are then sintered either in the solid state, or after partial or full melting of the metal. Sintering in the presence of a high fraction of liquid normally requires sintering to be performed in a container. When sintering in the fully solid state, it is more difficult to achieve bonding between the Al powder particles and sintering is usually aided by the addition of magnesium [5]. The final stage in this process is the removal of the template. In the case of salt, this is simply achieved by dissolution in warm water.

The main advantage of this process is that precise control over the volume fraction, size and morphology of the pores is possible, leading to foams with predictable and reproducible structures and mechanical properties. There are, however, some disadvantages to the process, in addition to problems with mixing and sintering. The size of parts that can be made in this way is limited, the porosity cannot be varied widely [3,4], the angular morphology of the salt particles is not ideal for an optimum balance of mechanical properties and removal of the salt from the preform can be very slow, particularly for large samples, affecting the rate at which parts can be made. For example, a part 35 mm in diameter and 80 mm in height, containing salt with a mean size between 338 and 1500 μm, took 4 h to remove the salt in hot water at 95 °C [4]. Removal of all the salt is critical as residual NaCl within the structure results in corrosion which is deleterious to the properties of the foam [3].

A possible solution to these problems is the use of porous, spherical salt beads. Large, porous salt spheres (3–7 mm in diameter) have been produced by mixing fine salt with water and flour and

* Corresponding author. Tel.: +44 115 9513744.
E-mail address: andrew.kennedy@nottingham.ac.uk (A.R. Kennedy).

0925-8388/$ – see front matter © 2010 Elsevier B.V. All rights reserved.
doi:10.1016/j.jallcom.2010.03.132

forming the resulting paste by hand [6]. This has the advantage that after the flour is removed, by heating at 400–500 °C, fine porosity exists within the spheres and water penetration into this porosity significantly increases their rate of dissolution [6]. This study details a novel process for the production of fine, porous salt beads and demonstrates their use in the production of porous Al by a powder metallurgical route.

2. Materials and methods

A flour and water paste was made by mixing 2 wt.% of glutinous rice flour in distilled water. To 10 cc of the paste, 50 g of salt (NaCl), with a particle size between 53 and 106 μm, was added and stirred until homogeneously mixed. The paste was poured into a beaker of vegetable oil and stirred at 1000 rpm, for 5 min, using a whisk. The oil was then heated from room temperature to 80 °C, whilst stirring. After reaching this temperature, heating and stirring were stopped, allowing the salt beads to settle to the bottom of the vessel. The beads were then sieved from the oil, cleaned in isopropyl alcohol, dried and then sieved to separate them into different size fractions. Salt beads (between 1.4 and 2.0 mm in diameter) were sintered at 755 °C, in air, for 12 h. En route to the sintering temperature the beads were held at 500 °C for 1 h to burn off the flour.

The tap density of the salt beads was determined a using an Autotap™ particle density analyser (Quantachrome) the density and porosity in the sintered spheres was measured using a combination of gas pycnometry (Micromeritics, AccuPyc 1330) and mercury intrusion porosimetry (Micromeritics, AutoPore IV). The morphology of the NaCl beads was characterised using optical microscopy and scanning electron microscopy (SEM).

Sintered salt beads (1.4–2.0 mm in diameter) were poured into a 22 mm diameter steel die with the bottom punch in place. The beads were tapped using the Autotap™ instrument to increase the packing fraction. An Al–1 wt.% Mg–0.5 wt.% Si–0.2 wt.% Cu alloy powder (with an average particle size of 116 μm), containing 1.5 wt.% wax to improve compaction, was poured on top of the salt bed and vibrated until it had completely percolated into the gaps between the salt particles. The resulting mixture was then cold compacted using a pressure of 250 MPa. The consolidated preform was sintered at 650 °C (just below the melting point) for 60 min in a tube furnace under flowing nitrogen. The density of the cellular metal can be controlled, to some degree, by the quantity of Al powder added and the degree of compaction of the resulting tapped mixture. An exhaustive investigation of the influence of these parameters is beyond the scope of this study, which simply aims to give a single example of the product generated by this process. In this example 4.6 g of Al alloy powder was tapped into a bed of 12 g of salt beads.

The resulting parts had the salt removed by immersion in static water held at 60 °C. Samples were sectioned using electro-discharge machining and examined using SEM. The density of the part, before and after removal of the salt, was calculated from the mass and volume of cylindrical samples. Mechanical testing was performed on parts that were 22 mm in diameter and 20 mm high. An Instron mechanical testing machine was used to determine the compression behaviour, following as closely as possible the Japanese standard, JIS H 7902, September 2008.

3. Results and discussion

In the preparation and processing of the paste, the flour acts as a binding agent. Water in the paste ensures that it is lipophobic and that spherical beads are formed when the paste is mechanically disintegrated. The optimum flour content of roughly 2.0 wt.% gives sufficient binding when needed, but not too viscous a paste that it cannot be broken up when stirred under the imposed conditions. The salt particles are bound together in the paste, and in the droplets, by the partial dissolution of the salt in the flour–water mixture. Heating the beads in the oil increases their rigidity, through partial gelatinisation of the starch in the flour (a process which takes place between roughly 60–80 °C for amylopectin, the principal starch present in glutinous rice) and by the removal of water from the paste. The increased rigidity prevents the beads from agglomerating and helps them retain their spherical shape after stirring has ceased.

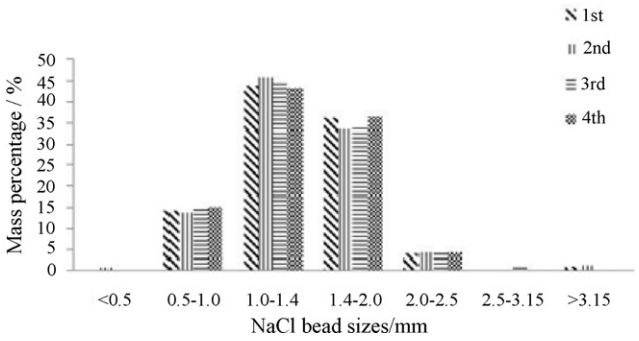

Fig. 1. NaCl bead size distribution for 4 identical process runs.

Fig. 1 presents the mass fractions of beads collected for different sieve sizes, for 4 production runs under identical processing conditions. Beads are produced with sizes ranging from 0.2 to 3.5 mm with a modal bead size between 1.0 and 1.4 mm. It can be seen that the reproducibility is good with less than a ±4% variation in values across all the sieve sizes.

Fig. 2 shows the typical structure of the beads that are produced by this method. The SEM image in Fig. 2b shows more clearly that the beads are spherical and that they have a rough surface, a result of being composed of angular salt particles. Fig. 3a and b shows higher magnification images of the salt bead surfaces. It can be seen that after sintering, the flour is burnt out leaving behind porosity. Sintering between the individual salt particles takes place, evidenced by rounding-off of the edges and faces of the angular salt particles and neck formation. For these small particles material transport is most likely to be via grain boundary diffusion, leading to some densification of the bead [7,8].

Mercury intrusion porosimetry of the sintered beads indicated that there were very few pores smaller than 5 μm in diameter, with most of the pores being between 10 and 33 μm in diameter. This measurement is in-keeping with the scale of the surface pores observed in the SEM image in Fig. 3b. The cumulative intrusion plot for a bed of salt beads is shown in Fig. 4. The density of the salt beads, measured by porosimetry at low intrusion pressure, was 1.8 g cc^{-1}. The skeletal density, measured at the highest intrusion pressure, and the density measured by gas pycnometry, were both

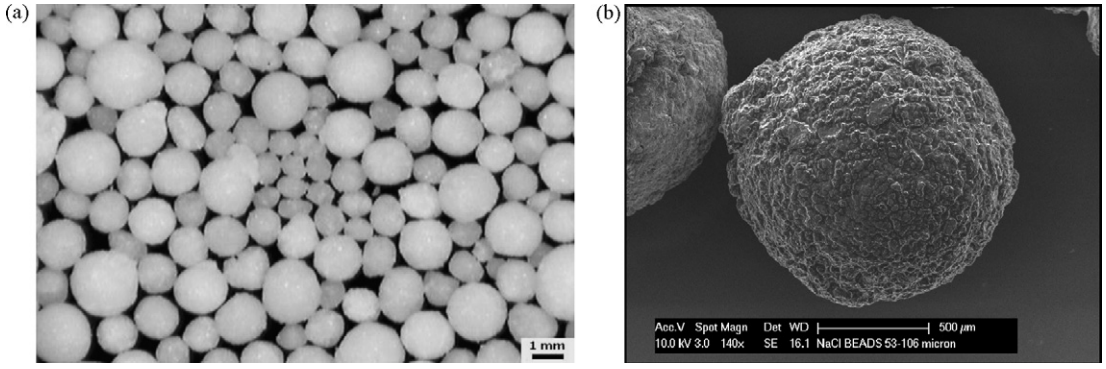

Fig. 2. The typical structure of as-made salt beads.

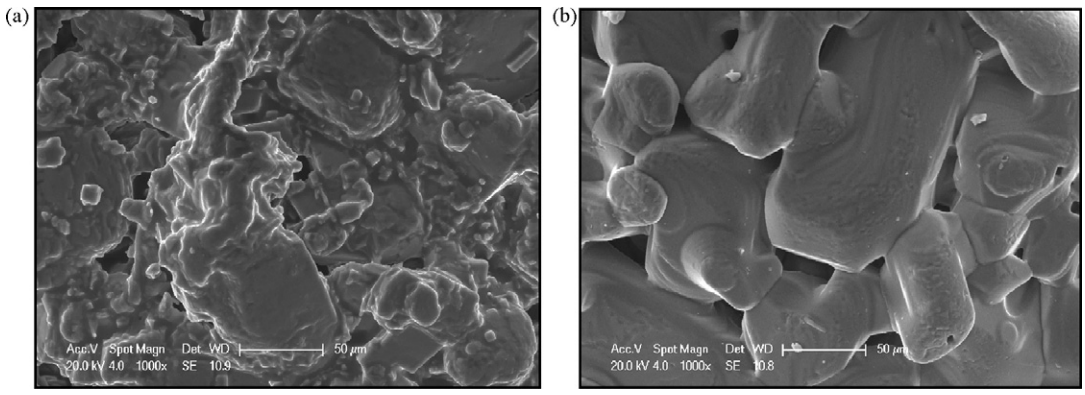

Fig. 3. SEM images of the surface of (a) as-made beads and (b) beads sintered at 755 °C for 12 h.

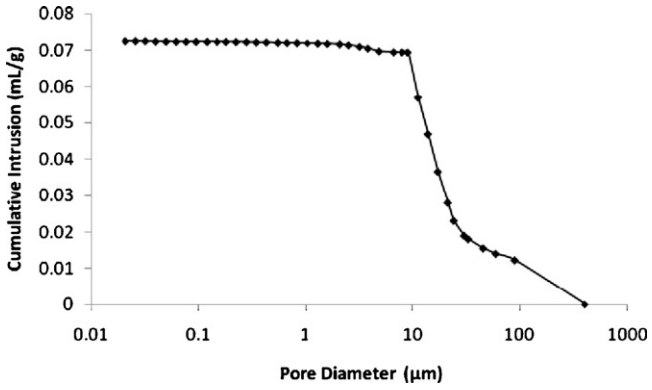

Fig. 4. Cumulative mercury intrusion plot for sintered salt beads.

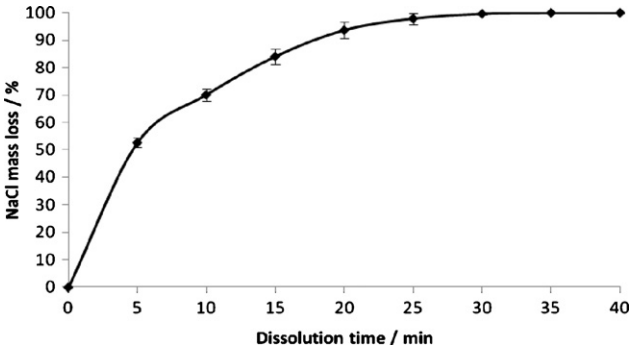

Fig. 5. Dissolution behaviour for salt beads in a sintered compact immersed in water at 60 °C.

2.15 g cc^{-1}, the same as the theoretical bulk density for salt. This indicates that the beads are roughly 84% dense and contain fully connected porosity. The tap density for these beads was 1.05 g cc^{-1} and therefore the volume percentage of beads in the packed bed is 58%.

After the Al alloy powder was tapped into beds of salt beads, the powder mixtures were compacted to an average density of 2.14 g cc^{-1} (with a standard deviation of 0.02 g cc^{-1} for 8 samples) and after sintering, the compacts expanded slightly, decreasing in density to 2.06 g cc^{-1} (with a standard deviation of 0.02 g cc^{-1}). The low standard deviations highlight the good reproducibility offered by this process which is achieved through precise control of the masses of powders and the compaction pressure.

The dissolution behaviour of the salt from the sintered (22 mm diameter) aluminium alloy compact in static water held at a constant 60 °C is shown in Fig. 5. More than 50% of the salt, by mass, is removed in the first 5 min and all the salt removed after roughly 30 min. This removal rate is much faster than is observed for monolithic salt (4 h is required at 95 °C for complete salt removal from 35 mm diameter samples [4]).

After dissolution of the salt, the resulting foams have an average density of 0.57 g cc^{-1} (with a standard deviation of 0.005 g cc^{-1}) and a relative density of 0.21. This indicates that the packing fraction of the salt beads must increase (as well as that of the metal powder) during compaction. Fig. 6 shows the macrostructures of cellular Al components. Through precise metering of the amount of Al powder, the gaps between the salt beads in the preform are sufficiently well filled for a continuous network of Al to be formed. The sectioned view shows that there is very little excess Al powder on either the top or bottom surfaces.

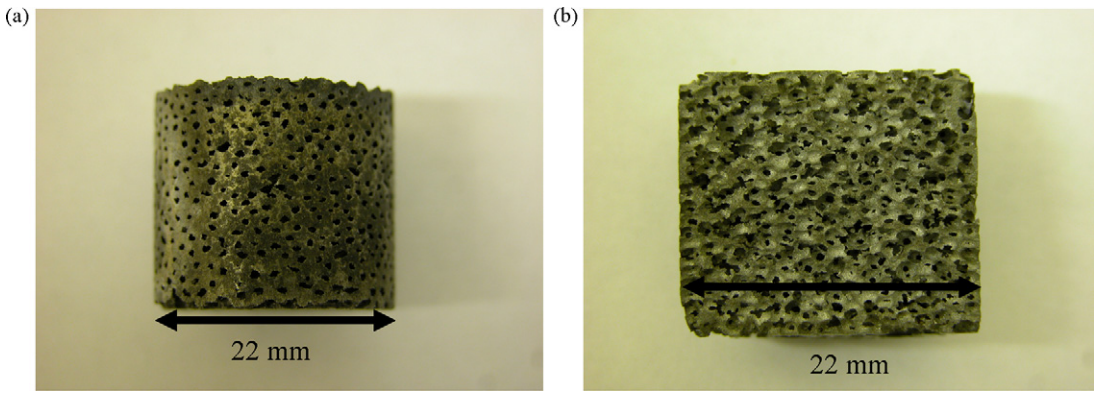

Fig. 6. Cellular Al showing (a) the rear view and (b) a view of a section at the mid-plane.

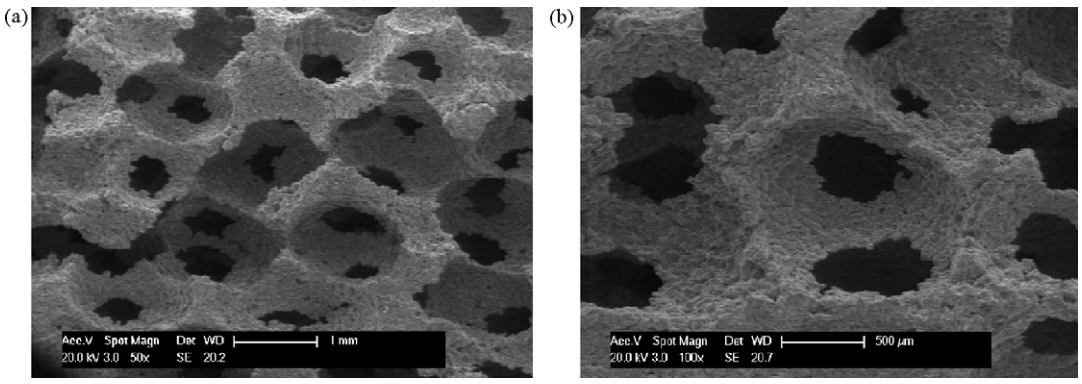

Fig. 7. SEM images showing the cell structure and porosity within the cell walls.

Fig. 7 shows the pore morphology more clearly and that the pores remain spherical after compaction and are connected by small windows. These windows arise due to incomplete filling of the cavities between the salt beads, due to the inability of Al powder particles to fit into the small spaces at the contact points between neighbouring salt spheres. A simple mathematical analysis for two, touching, 1.7 mm diameter spheres shows that for an "infiltrating" particle of 116 μm, a region roughly 500 μm in diameter around the contact point cannot be filled. This is similar to the size of the windows observed in Fig. 7. The number of windows per pore depends on the coordination number for the packed structure, which is likely to be between 6 and 9 for packing of this type [7]. Fig. 7b also reveals that the cell walls themselves are porous as a result of incomplete sintering. It is also apparent in Fig. 7 that there are a number of incomplete cell walls. Whilst some of these defects may have been introduced during sectioning of the thin, fragile struts, they may also have arisen due to incomplete filling of the gaps between the salt particles during the tapping stage.

Fig. 8 presents three stress–strain curves for compression testing of these foams. Although there are some undulations in the trace, a reasonably constant plateau stress is observed, varying between 1 and 2 MPa; a characteristic which is preferred for an energy absorber. This behaviour is atypical of similar foams made using angular or spherical dense salt particles [9–11] and when irregular pores are observed [12], when a steady increase in stress with strain is observed after yielding. It is possible that the reasonably constant plateau stress is a result of the porous and brittle nature of these sintered powder structures and that the undulations are due to structural inhomogeneities arising from incomplete cell walls. A more detailed investigation is, however, required to characterise the structure and defects and to determine why the compression behaviour should differ from such similar materials as those reported in [9,11,12].

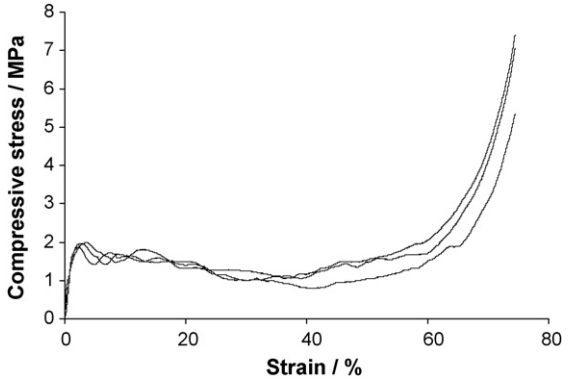

Fig. 8. Stress–strain curves for cellular aluminium with a density of 0.57 g cc^{-1}.

The 0.2% proof stress and stiffness for the foam are 1.92 MPa and 0.46 GPa respectively (with standard deviations of 0.06 MPa and 0.03 GPa respectively for 4 samples). These small variations in properties are a result of the small scatter in relative density. Foams with similar relative densities made by infiltration of beds of finer salt particles with molten pure aluminium [13,14] showed proof stresses in the range 0.5–1.0 MPa and stiffnesses in the range 1–1.5 GPa. The differences presumably arise from higher strength of the alloy powder used in this study and from the porosity present in the cell walls. Porosity in PM materials is much more detrimental to the stiffness than the strength in compression [15] and results in a much larger decreases in stiffness than is predicted by established relationships between porosity and stiffness for foams [15,16]. It is, therefore, to be expected that the foam stiffness will be lower than that for a foam with an equivalent relative density and fully dense struts.

4. Conclusions

A novel process has been demonstrated for the manufacture of spherical salt beads with sizes between 0.5 and 3.0 mm using a flour-based paste which is mechanically disintegrated in oil. The process has been shown to be repeatable. After thermal decomposition of the flour from the beads they contain a high fraction (16%) of interconnected porosity.

Tapped beds of salt beads have been partially filled with an Al alloy powder using vibration. The fine Al powder penetrates the gaps between the salt beads, preserving the structure of the tapped bed, and is a highly attractive alternative to powder mixing methods.

After compaction and sintering, and dissolution of the salt, a highly porous component is produced. The porous nature of the beads, which allows water to penetrate them results in rapid dissolution of the salt from the component.

Cellular aluminium parts can be produced with very small deviations in density due to the control that is possible over the mass fractions of powders that are used and the compaction conditions. The reproducibility in the density results in reproducible mechanical properties.

Acknowledgements

The authors are grateful for financial support from the British Council in the PMI2 Connect programme.

References

[1] J. Banhart, Prog. Mater. Sci. 46 (2001) 559–632.
[2] Y.Y Zhao, D.X. Sun, Scripta Mater. 44 (2001) 105–110.
[3] Y. Zhao, F. Han, T. Fung, Mater. Sci. Eng. A364 (2004) 117–125.

[4] G. Hao, F. Han, W. Li, J. Porous Mater. 16 (2009) 251–256.
[5] G.B. Schaffer, T.B. Sercombe, R.N. Lumley, Mater. Chem. Phys. 67 (2001) 85–91.
[6] R. Goodall, A. Mortensen, Adv. Eng. Mater. 9 (2007) 951–954.
[7] R.M. German, Sintering Theory and Practice, Wiley–Interscience Publication, New York, 1996.
[8] R. Goodall, J.F. Despois, A. Mortensen, J. Eur. Ceram. Soc. 26 (2006) 3487–3497.
[9] R. Goodall, A. Marmottant, L. Salvo, A. Mortensen, Mater. Sci. Eng. A465 (2007) 124–135.
[10] C. San Marchi, A. Mortensen, Acta Mater. 49 (2001) 3959–3969.
[11] C. Gaillard, J.F. Despois, A. Mortensen, Mater. Sci. Eng. A374 (2004) 250–262.
[12] R. Surace, L.A.C. De Filippis, A.D. Ludovico, G. Boghetich, Mater. Des. 30 (2009) 1878–1885.
[13] J.F. Despois, A. Marmottant, L. Salvo, A. Mortensen, Mater. Sci. Eng. A462 (2007) 68–75.
[14] R.D. Goodall, J.-F. Despois, A. Marmottant, L. Salvo, A. Mortensen, Scripta Mater. 54 (2006) 2069–2073.
[15] X. Deng, G.B. Piotrowski, J.J. Williams, N. Chawla, Int. J. Fatigue 27 (2005) 1233–1243.
[16] L.J. Gibson, M.F. Ashby, Cellular Solids, Cambridge University Press, Cambridge, 1997.